

Room-temperature stimulated emission from ZnO multiple quantum wells grown on lattice-matched substrates

Takayuki MAKINO, Yusaburo SEGAWA,
Masashi KAWASAKI^{a)} and Hideomi KOINUMA^{b)}.

October 16, 2018

Abstract

The optical properties of ZnO quantum wells, which have potential application of short-wavelength semiconductor laser utilizing a high-density excitonic effect, were investigated. Stimulated emission of excitons was observed at temperatures well above room temperature due to the adoption of the lattice-matched substrates. The mechanism of stimulated emission from ZnO quantum wells is discussed in this chapter.

affiliations:

Photodynamics Research Center, RIKEN (Institute of Physical and Chemical Research)
(519-1399, Aramaki aza Aoba, Aobaku, Sendai 980-0845)

E-mail: tmakino@postman.riken.go.jp

a) Institute for Materials Research, Tohoku University,
(Sendai 980-8577, Japan)

b) Frontier Collaboration Research Center, Tokyo Institute of Technology
(4259 Nagatsuda, Midoriku, Yokohama 226-8503)

1 Introduction — ZnO as an optoelectronics material

There have been many studies recently on the properties of widegap semiconductors aimed at the development of a short-wavelength laser diode. Akasaki and Nakamura developed a blue light-emitting diode and a continuous-wave laser in which InN–GaN alloys play an essential role as the active layers [1, 2]. However, in all commercially available semiconductor lasers including GaN-lasers, a recombination of electrons and holes is used as the mechanism of laser action. In such cases, the threshold carrier density required to accomplish the inversion distribution of a population for an electron–hole system is one or two orders of magnitude higher than the Mott transition density. If an exciton-related recombination is used as the mechanism of laser action, the resultant threshold value is expected to be two or three orders of magnitude lower with higher quantum efficiency. Because of this expectation, interest has recently been shown in zinc oxide (ZnO), the band gap of which is in the ultraviolet range. In addition, the exciton binding energy (EBE) of ZnO is rather large (60 meV) compared with those of other semiconductors such as group II-selenides or group III-nitrides. Thus, the advantage of ZnO is that excitons can exist stably even at room temperature (RT) and even under a high-density condition.

Atomic layer control technology in the laser-assisted molecular-beam-epitaxy (LMBE) of oxides has advanced remarkably since the discovery of high-temperature superconductors. In response to this, we started study of ZnO epitaxial growth for the development of the short-wavelength semiconductor optoelectronics. At first, we adopted sapphire as substrates that had large lattice-mismatch (18%) with ZnO. Optical and structural properties of ZnO epitaxial layers deposited on sapphire has been investigated. These studies revealed that the ZnO epilayers are adapted for the optoelectronic applications with the following aspects:

1. Laser oscillation of excitonic origin was observed at room-temperature. Grain boundaries in the epilayers act as longitudinal cavities.
2. Band gap energies can be tuned by preparing the (Zn,Mg)O and (Zn,Cd)O solid solutions [3, 4, 5].
3. Growth of ZnO/(Mg,Zn)O multi-quantum wells (MQWs) were succeeded.
4. Optical properties of these MQWs were investigated. Excitonic luminescence accompanied by the quantum size effect at low temperatures was observed [6, 7, 8].

However, the abovementioned studies have also revealed some problems (unsatisfactory properties of ZnO epilayers) that are unavoidable as long as lattice-mismatched substrates are used. These ZnO thin films are indeed epitaxial but stay multicrystalline in nature having incoherent grain boundaries. These grain boundaries seem to be useful for observing the excitonic laser action because they can function as mirrors of a longitudinal cavity. The electrical properties of such films are, however, rather poor, as represented by a typical electron concentration of $n \sim 10^{17} \text{ cm}^{-3}$ and a typical Hall mobility of $\mu \sim 10 \text{ cm}^2/\text{V s}$ at room temperature. The electrical properties of the epilayers are clearly inferior to those of bulk single crystals ($n \sim 10^{15} \text{ cm}^{-3}$ and $\mu \sim 200 \text{ cm}^2/\text{V s}$). The crystallinity of epilayers is also inferior. In addition, the fact that neither luminescence (photoluminescence) nor a stimulated emission could be observed at room temperature in MQWs grown on the sapphire substrates is a problem. The current advanced technology of compound semiconductors cannot be fully utilized in the case of such inferior thin films and quantum wells (QWs). Thus, QWs of higher quality must be developed to produce laser-diodes that can oscillate with a lower threshold. Furthermore, *n*- and *p*-type layers that have both high mobility and low resistance must be formed in order to perform current injection efficiently.

These problems might be resolved by using lattice-matched substrates. We have adopted hexagonal ScAlMgO₄(0001) with lattice constants of $a = 3.246 \text{ \AA}$ and $c = 25.195 \text{ \AA}$ (Ref. [9]) that have an in-plane lattice mismatch as small as 0.09%. ScAlMgO₄ is regarded as a natural superlattice composed of alternating stacking layers of wurtzite-type MgAlO_x and rocksalt (111)-ScO_y layers and hence has a cleavage habit along the (0001) plane. High-quality single crystals can be grown by Czochralski’s method. The structure of a crystal grown by this method and a possible hetero-interface with ZnO are schematically shown in Fig. 1 of Ref. [10].

Although there is now a fairly good understanding of the basic properties of ZnO epilayers, it is only recently that the basic properties of its QWs have been studied in detail. For example, Vispute *et al.* reported the growth and optical properties of GaN/ZnO/GaN double heterostructures. Although the combination of ZnO and (Zn,Mg)O has been used in a study by another research group (Chen *et al.* [11]), more comprehensive studies on this interesting and unexplored material have been conducted by us. In this paper, we describe the optical properties of ZnO/(Zn,Mg)O MQWs grown on lattice-matched ScAlMgO₄ (SCAM) substrates in detail. This chapter is organized as follows. The experimental procedures are briefly described in Sect. 2. Improvements in various properties of ZnO thin films achieved by the use of the lattice-matched substrates are described in Sect. 3. In Sects. 4–7, quantum confinement effects of excitons, the well-width dependence of the exciton-phonon coupling constants, and possible mechanism of a stimulated emission of ZnO MQWs are described respectively. The summarizing remarks are given in Sec. 8.

2 Method for growing MQW samples

Samples of MQWs (10 periods) were grown by the method of laser molecular-beam epitaxy. A QW is defined as stacks alternatively deposited by using two kinds of very thin semiconductor layers (wells and barriers) that have different band gap energies. ZnO was used as a well layer material and a ZnMgO solid solution, the band gap of which is larger than that of ZnO, was used as a barrier layer. The Mg concentration dependence of the band gap energy is given elsewhere [12]. It should be noted that the in-plane lattice mismatch between ZnO and these alloys is very small. The Mg concentration was set to 0.12 or 0.27, because the barrier height could be changed by a change in its concentration. Eighteen samples with different Mg concentrations and well widths (L_w), 6.9 to 46.5 Å, were prepared in order to estimate the L_w dependence of their optical properties. Barrier layer thickness was fixed at 50 Å. The samples were grown by the “combinatorial” method, the concept of which has been explained in the review article [13]. Readers should refer to related papers in which the apparatuses developed for efficient structural and optical characterizations are described [14, 15, 16, 17].

3 Improvements in properties of ZnO thin films achieved by the use of lattice-matched substrates

Here, we describe briefly the improvements in the properties of ZnO epilayers achieved by using lattice-matched SCAM substrates. Observation of the surface morphology of ZnO/SCAM epilayers revealed that the steps have a flat terrace in the scale of an atomic level and have a height of 0.26 nm (corresponding to the charge neutral unit). Comparison of the full width at half maximum (FWHM) of the x-ray diffraction (XRD) curves showed that the crystallinity of these epilayers had reached almost the same level as that of a single crystal [10]. These films also have high carrier mobility (100 cm²/Vs) and low residual carrier concentration (10¹⁵ cm³). Even if the growth temperature is lowered to about 200 °C, the high level of crystallinity was not changed. Recently, the formation of epilayers that have high resistance in which Hall measurement cannot be performed, and that have

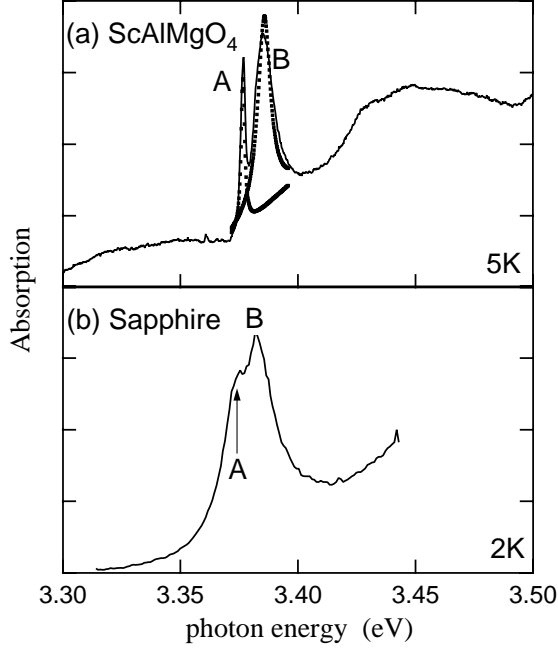


Figure 1: Comparison of low-temperature absorption spectra obtained from a ZnO epilayer grown on a sapphire substrate and that grown on a SCAM substrate [21]. Temperatures are shown on the right-hand side of the figure. SCAM is an abbreviation of ScAlMgO₄. “A, B” indicates A- and B-exciton absorption bands, and “I₆” shows PL of a bound exciton state.

the high mobility (≈ 200 cm²/Vs) has been achieved. In order to examine the activation efficiency of donor doping, *n*-type samples were prepared by doping aluminum. The activation efficiency was about 10 times greater than that of a thin film grown on a sapphire substrate. The optical properties of *n*-type ZnO:Al has been reported elsewhere [18]. In ZnO, the A-B exciton splitting is only 7 or 8 meV [19]. These two excitonic peaks were clearly resolved in the absorption spectrum measured at 4.2 K for bulk crystals [20]. On the other hand, this was not the case for ZnO epilayers grown on sapphire substrates [21] as shown in Fig. 1. The two excitonic peaks became too broad to be resolved because the damping constant of the excitons became larger due to the inferior crystallinity, as mentioned earlier. Such undesired broadening could be avoided in the case of ZnO epilayers grown on SCAM substrates. The FWHMs of the exciton absorption bands of these samples were similar to those of bulk crystals [20, 21]. It was confirmed that the threshold for the stimulated emission is also significantly improved [22]. Such improvements in electrical, structural and optical properties would not be possible if a sapphire substrate is used. It can be concluded that quality of these single-crystalline ZnO epilayers satisfies the stringent requirements for being regarded as compound semiconductors.

4 Quantum confinement effect of excitons in quantum wells

As mentioned earlier, the MQWs showed the following drawbacks due to the formation of rough interfaces caused by the use of lattice-mismatched substrates: (1) controllability of layer thickness is not sufficient for quantum confinement effect to be elicited in the case of $L_w \leq 15$ Å, and (2)

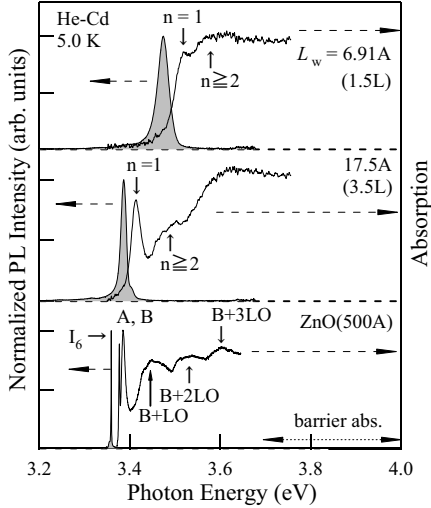


Figure 2: PL and absorption spectra obtained from ZnO/Mg_{0.12}Zn_{0.88}O MQWs measured at 5 K for L_w of 17.5 and of 6.9 Å. Absorption energy of barrier layers is shown by a horizontal arrow. Spectra obtained from a 500-Å-thick ZnO film are also shown. “B+LO, B+2LO, and B+3LO” correspond to exciton-phonon complex transitions, “ $n = 1$ ” shows the lowest excitonic absorption of the well layers, and “ $n \geq 2$ ” means the excited states of the exciton or higher interband transitions.

PL efficiency is not high enough to enable observation of the exciton emission at RT [6, 23]. These problems must be overcome for an optoelectrical device to be operable at RT. These problems, which were unavoidable when the sapphire substrates were used, could be eliminated by using ScAlMgO₄ substrates [24].

The XRD patterns of the MQWs showed Bragg diffraction peaks and clear intensity oscillations due to Laue patterns corresponding to the layer thickness. This indicates a high crystallinity and a high degree of thickness homogeneity. Furthermore, observation of the atomic force microscopy (AFM) images revealed that the surface of an MQW is composed of well-defined atomically flat terraces and steps corresponding to the charge neutral unit of ZnO. Therefore, the interface roughness in the heterostructure cannot be larger than 0.26 nm. We conclude that ZnO and MgZnO alloy layers grow in a two-dimensional growth mode on this substrate, resulting in the formation of a sharp hetero-interface between them.

Figure 2 shows PL and absorption spectra in ZnO/Mg_{0.12}Zn_{0.88}O MQWs on SCAM substrates measured at 5 K with well widths (L_w) of 17.5 and 6.9 Å. The PL and absorption spectra in a 500-Å-thick ZnO epilayer on a SCAM substrate are included for comparison. Both the PL and absorption peaks shifted towards the higher energy side as L_w decreased. This shift was due to the quantum confinement effect. The exciton Bohr radius is ≈ 18 Å [19]. The absorption peaks ($n = 1$) arise from the lowest excitonic states of well layers. The peak energies of PL were constantly located on the lower energy side of those of absorption peaks.

Figures 3(b)–(c) show the well width dependence of the peak energies of PL (closed circles) and absorption (open squares), respectively [24]. The lowest transition energy of excitons (open triangles) formed with confined electrons and holes was calculated by using the model of one-dimensional, finite periodic square-well potential proposed by Gol’dman and Krivchnokov [25]. The EBE (59 meV,

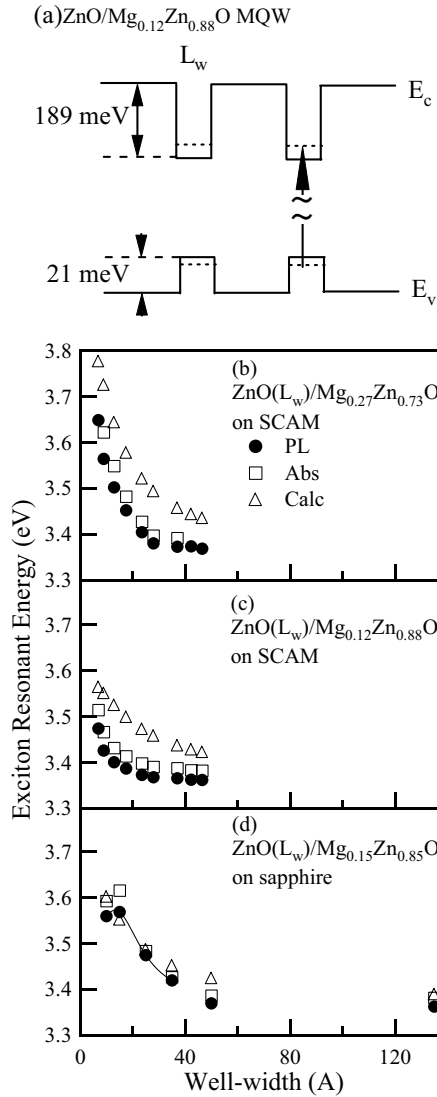


Figure 3: (a) Diagram of conduction and valence bands between barrier and well layers in a ZnO/Mg_{0.12}Zn_{0.88}O MQW [6]. The upward arrow shows the lowest interband transition. (b) Peak energies of PL (circles) and absorption (squares) are plotted against L_w in [ZnO/Mg_{0.27}Zn_{0.73}O]₁₀ on SCAM substrates. Results of calculation (triangles) of the interband transition energy that include the excitonic effect are also shown. (c) Similar except that the Mg content was $\approx 12\%$. (d) Similar except that the substrate was sapphire. The Mg content was $\approx 15\%$. Energies of PL excitation spectra (squares) are plotted instead of those of absorption spectra, due to the presence of 100-nm-thick ZnO buffer layers. Note that the peak energies of PL excitation spectra coincide with those of the absorption spectra. The curve is a visual guide [24].

Ref. [26]) is assumed to be independent of L_w here, although, as will be shown later, EBE actually depends on L_w . The optical transition process on ZnO/Mg_{0.12}Zn_{0.88}O MQW is shown in Fig. 3(a). This tendency of the L_w dependence of the exciton transition energy was qualitatively reproduced by calculation. As reported by Coli and Bajaj [27], incorporation of the effects of exciton-phonon interaction and quantum confinement in the calculation of the EBE, leads to the values of the excitonic transitions that agree well with our experimental data. Figure 3(d) shows the corresponding peak energy plot for MQWs grown on sapphire substrates. As seen in Fig. 7(d), both of the peak energies have a maximum at L_w of 15 Å when sapphire substrates were used. This is a critical L_w that prevents quantum confinement with respect to the exciton energy. This is because of the poor controllability of L_w due to the lattice mismatching.

5 Well-width dependence of exciton-phonon interaction in quantum wells

The coupling constant between excitons and phonons in ZnO MQWs has not been estimated quantitatively. We therefore tried to quantify the coupling constant by estimating the temperature dependence of the absorption spectra. Figure 4 shows the temperature dependence of the full width at half maximum (FWHM) of the excitonic absorption peaks for a ZnO epilayer (a) and for a typical MQW sample with a QW width of 17.5 Å (b). The solid line represents the fitted results based on the following equation. The temperature dependence of the FWHM can be approximately described by the following equation [28]:

$$\Gamma(T) = \Gamma_0 + \gamma_{\text{ph}}T + \Gamma_{\text{LO}}/[\exp(\hbar\omega_{\text{LO}}/k_{\text{B}}T) - 1], \quad (1)$$

where Γ_0 , $\hbar\omega_{\text{LO}}$ (72 meV), γ_{ph} , Γ_{LO} and k_{B} are the inhomogeneous linewidth at temperature (T) of 0 K, longitudinal optical (LO)-phonon energy, strengths of the exciton-acoustic-phonon and the exciton-LO-phonon couplings and the Boltzmann constant, respectively. It was experimentally found that $\hbar\omega_{\text{LO}}$ of the MQWs is not different from the bulk value.

Figure 5 (closed circles, left axis) shows the values of Γ_{LO} obtained for the epilayer and its well-width (L_w) dependence obtained for ZnO/Mg_{0.12}Zn_{0.88}O MQWs. The values of Γ_{LO} of the MQWs are smaller than those for the epilayers and monotonically decrease with decrease in L_w . Here we try to explain this result by the enhancement of EBE induced by the quantum confinement effect. Figure 5 (open circles, right axis) shows L_w dependence of EBE. This dependence was determined by studying spectra of stimulated emission. As is well known, the major process that contributes to broadening of the exciton linewidth is scattering of 1S excitons into free-electron-hole continuum or into excited excitonic states by absorbing LO phonons. If EBE exceeds $\hbar\omega_{\text{LO}}$ (72 meV), dissociation efficiency into the continuum states is greatly suppressed compared to the case of EBE smaller than $\hbar\omega_{\text{LO}}$. In such case, Γ_{LO} is reduced. Indeed, EBE exceeds $\hbar\omega_{\text{LO}}$ in the case of MQWs. A similar effect has also been observed in other QW systems [29]. Schematic explanation is described in detail in corresponding original papers [30, 31].

6 The localization mechanism of the exciton in a quantum well

It was found that the excitonic luminescence in the ZnO MQWs under investigation is due to radiative recombination from excitons localized by the potentials formed by the fluctuations of L_w and barrier height. Our spectral assignment are based on (1) the well width dependence of Stokes shift (difference

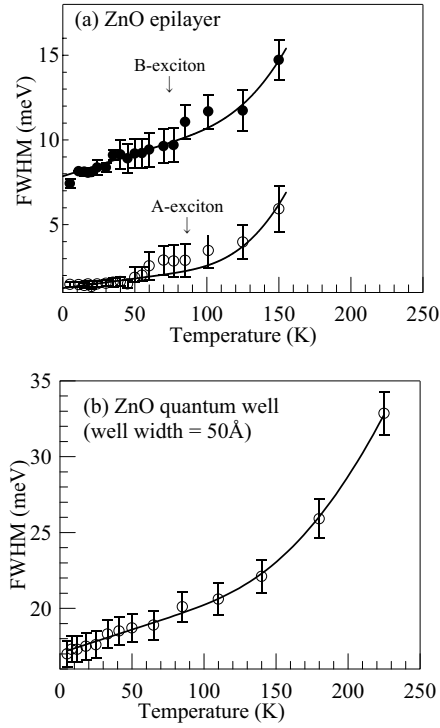


Figure 4: (a) Width (full width at half maximum, circles) of *A*- and *B*-exciton absorption bands plotted as a function of temperature. Closed circles are data of the *A*-excitons and the open circles are data of the *B*-excitons. The solid curves represent the fitting results. (b) Similar plot for the MQW with Mg concentration of 0.12 and L_w of 46.5Å [21, 30].

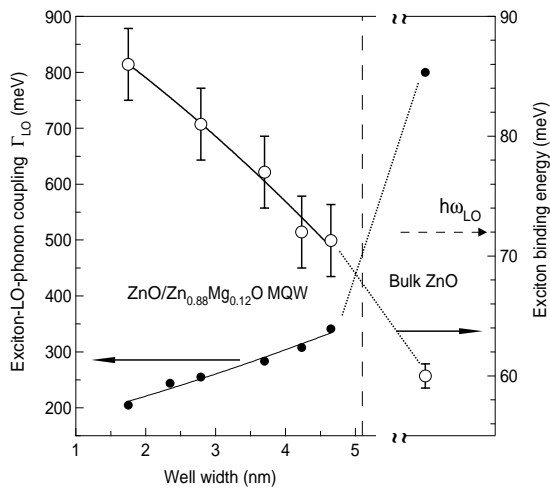


Figure 5: Strengths of coupling between excitons and LO phonons Γ_{LO} (closed circles) and exciton binding energies (open circles) in bulk ZnO and MQWs with different L_w s [37]. The solid curve is a visual guide.

between the energies of absorption and luminescence bands), (2) the temperature dependence of PL spectra, and (3) the spectral distribution (luminescence energy dependence) of decay time constants of luminescence [24, 32, 30, 33]. A typical example of the spectral distribution of decay time constants is shown in the lowest curve of Fig. ??(b). Here, the temperature dependence of the PL spectrum in a QW in the case of magnesium composition of 0.27 is described in detail.

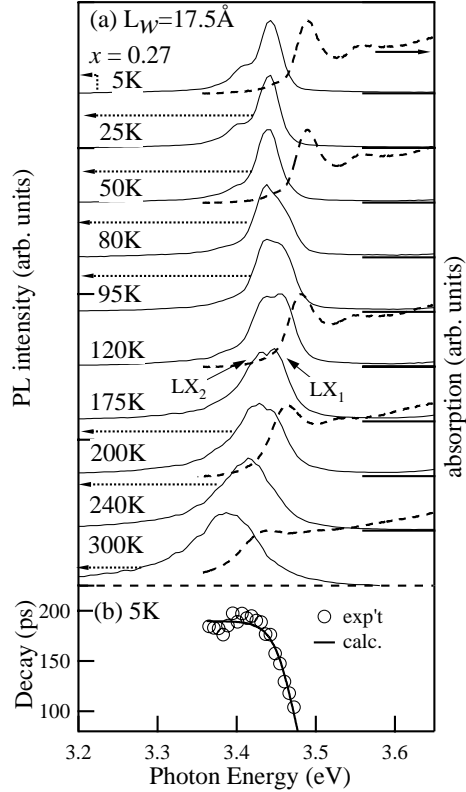


Figure 6: (a) PL (solid line) and absorption (broken line) spectra in a ZnO (17.5 Å)/Mg_{0.27}Zn_{0.73}O MQW over the temperature range of 5 to 300 K. All of the spectra have been normalized and shifted in the vertical direction for clarity. (b) PL decay times as a function of monitored photon energy at 5 K in the same MQW. The dotted curve is results of the theoretical calculation based on the model of the excitonic localization.

Figure 6(a) shows the temperature dependence of PL (solid line) and that of absorption (broken line) spectra in ZnO(17.5 Å)/Mg_{0.27}Zn_{0.73}O MQWs over a temperature range of 5 to 300 K. It should be noted that spectra obtained at temperatures between 95 and 200 K had two peaks, both of which originated from a recombination of localized excitons. The separation of these peaks was 12 to 20 meV. Figure 6(b) shows PL decay time as a function of monitored photon energy at 5 K in the same MQW. The dotted curve is the results of theoretical calculation based on the model of the excitonic localization [24, 34]. Figure 7(a) summarizes peak energies of the PL spectra (E_{PL}^{pk}) (solid circles and triangles) and the excitonic absorption energy (solid squares) as functions of temperatures. It should be noted that the higher PL peak position does not coincide with that of absorption spectra even at temperatures near room temperature. We also examined, for comparison, the temperature dependence of PL peak energy in an MQW having a lower barrier height: a ZnO/Mg_{0.12}Zn_{0.88}O

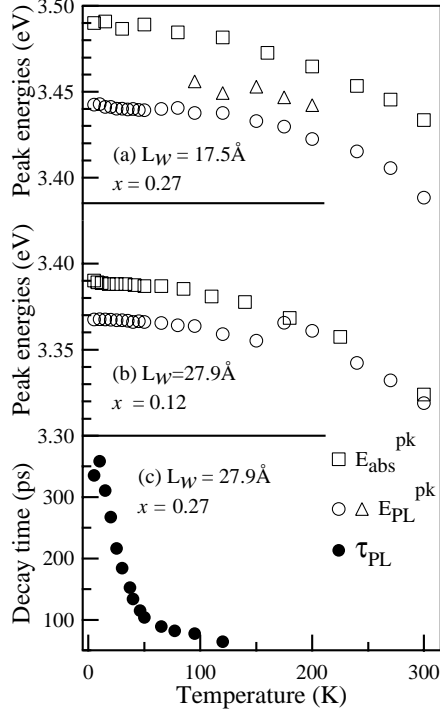


Figure 7: PL (solid circles and triangles) and absorption (solid squares) peak positions as a function of temperature in ZnO(17.5 Å)/Mg_{0.27}Zn_{0.73}O (a) and ZnO(27.9 Å)/Mg_{0.12}Zn_{0.88}O (b) MQWs. (c) Temperature dependence of PL decay times, τ_{PL} , in ZnO(27.9 Å)/Mg_{0.27}Zn_{0.73}O MQWs at temperatures of 5–120 K [24].

MQW with a well width of 27.9 Å. Figure 7(b) shows the peak energies of PL (circles) and absorption (squares) spectra in this sample. In this case, the energies of luminescence and absorption are the almost same with each other at temperatures near room temperature. Two kinds of MQWs having different barrier heights showed significantly different temperature dependences of PL spectra.

Following a temperature rise, the PL energy of ZnO(17.5 Å)/Mg_{0.27}Zn_{0.73}O MQWs exhibited low energy shifts between 5K and 50K, blue-shifts between 50 and 200 K, and again shifts to a low energy side at temperatures higher than 200 K. Furthermore, at temperatures between 95 and 200 K, the spectra had two peaks, both of which originated from a recombination of localized excitons. The absorption peak energies both in ZnO epilayers and in MQWs are monotonically decreasing functions of temperature as was revealed in previous studies [21, 30]. This is attributed to the temperature-induced shrinkage of the fundamental energy gap.

In general, when a dominant PL peak is assigned to a radiative recombination of localized excitons, its peak energy blue-shifts with increase in temperature in a range of low temperatures and red-shifts at higher temperatures. The E_{PL}^{pk} blue-shifts and continuously connects to that of free excitons due to thermal activation of localized excitons. The E_{PL}^{pk} of the free-excitonic emission is a monotonically decreasing function of temperature due to the band gap shrinkage. The temperature dependence shown in Fig. ??(a) is, however, different from the abovementioned typical behavior. The temperature dependence of the recombination mechanism for localized excitons is thought to be closely related to the temperature variation in the decay time constant of their PL. Thus temperature dependence of

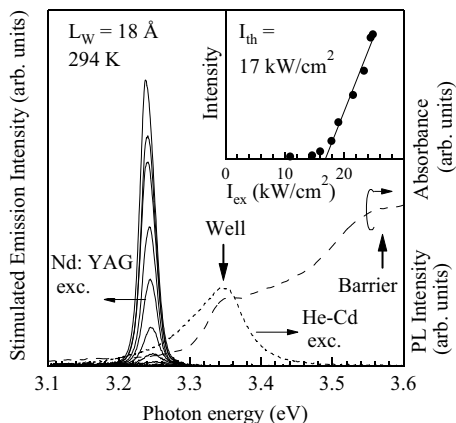


Figure 8: Excitation intensity (I_{ex}) dependence of the stimulated emission spectra obtained from a ZnO/Mg_{0.12}Zn_{0.88}O SL ($L_w=1.8$ nm) under the condition of pulsed excitation at RT. Spontaneous PL (dotted line) under the condition of continuous-wave (cw) excitation and absorption (broken line) spectra are also shown. Inset shows the integrated intensity of the stimulated emission peak as a function of I_{ex} . Threshold intensity (I_{th}) is 17 kW/cm² [36].

PL decay times (τ_{PL}) in an MQW with a L_w of 27.9 Å is shown in Fig. 7(c). The τ_{PL} values exhibit nonmonotonical behavior with respect to temperature; the value increased in a low temperature range and decreased above a certain critical temperature.

The temperature dependence of the recombination mechanism for localized excitons can be explained [35] as follows. For 5 K $< T < 50$ K, the relatively long relaxation time of excitons gives the excitons more opportunity to relax down into lower energy tail states caused by the inhomogeneous potential fluctuations before recombining. This is because radiative recombination processes dominate in this temperature range. This behavior produces a red-shift in the peak energy position with increasing temperature. For 50 K $< T < 95$ K, the exciton lifetimes decrease with increasing temperature. Thus, these excitons recombine before reaching the lower energy tail states. This behavior enhances a broadening of the higher-energy side emission and leads to a blue shift in the peak energy. (iii) For 95 K $< T < 200$ K, further enhancement of high-energy emission components produces a new peak, as seen in Fig. 7(a) (triangles). (iv) At temperatures above 200 K, since the excitons are less affected by the temperature-induced rapid change in their lifetimes and since the relaxation rate of the excitons increased due to an increase in the phonon population, blue-shift behavior becomes less pronounced. Since the energy of a blue-shift is less than the temperature-induced band gap shrinkage, the peak position again exhibits a red-shift behavior. As mentioned above, the features of excitonic spontaneous emission in the well layers are sensitively affected by the dynamics of recombination of localized exciton states, which significantly vary with temperature. Readers should refer to the original articles for details [32].

7 Mechanism of stimulated emission in multiple quantum wells

As shown in Fig. 8, the energies of spontaneous PL and absorption peaks are almost the same at room-temperature [24]. The spontaneous emission spectrum was obtained under the condition of excitation using a 5-mW-power helium cadmium laser operated in the continuous-wave mode, while the stimulated emission spectrum was obtained under the condition of high-power excitation using a frequency-tripled mode-locked Nd:YAG laser (355 nm, 10 Hz, 15 ps) operated in the pulsed mode. The power of excitation was varied, as is described later. The agreement between the spontaneous emission and absorption peaks is an indication of the well-regulated heterointerfaces as well as the small compositional fluctuations in the barrier layers (well-depth fluctuations). Such room-temperature PL in the MQWs grown on the sapphire substrates was not found.

We performed high-power excitation experiments to determine the characteristics of stimulated emission in ZnO MQWs in the optical pumping mode. Figure 8 shows stimulated emission spectra of MQWs with $x = 0.12$ and $L_w = 17.5 \text{ \AA}$ that were obtained at room temperature. Strong and sharp emission peaks were observed at 3.24 eV above a very low threshold ($I_{th}=17 \text{ kW/cm}^2$), and their integrated intensities rapidly increased as the excitation intensity (I_{ex}) increased, as can be seen in the inset. Although such stimulated emission was not observed even at 4.2 K in the case using a sapphire substrate, RT stimulated emission in MQWs studied here was observed. This is one of the significant improvements achieved by applying lattice-matching conditions to a substrate.

The L_w dependences of peak energies of the absorption and stimulated emissions are summarized in Fig. 9. Similar dependence of the threshold is also shown in Fig. 9(c). The stimulated emission energy is 100 meV lower than that of the absorption peak. The lowest threshold value was 11 kW/cm^2 in the case of L_w of 47 \AA .

We tested the high-temperature operation of the stimulated emission from the viewpoint of possible applications to devices. Figure 10 shows the temperature dependence of the $I_{stim} - I_{ex}$ curves of a MQW with $x = 0.26$ and $L_w = 4.2 \text{ nm}$ in the temperature range of 294 K to 377 K. Here, I_{stim} is the intensity of the stimulated emission and I_{ex} is the excitation intensity. The threshold of the stimulated emission (I_{th}) increased gradually with increasing temperature. The inset shows the temperature dependence of I_{th} on a logarithmic scale. Characteristic temperature, which is an index of stability of threshold characteristics with respect to temperature rise, was estimated to be 87 K [36]. This was significantly higher than that of a 55-nm-thick ZnO/sapphire (67 K) [22], which showed excitonic laser action with a threshold of 24 kW/cm^2 . We speculate that this kind of improvement can be explained by the enhanced binding energy of excitons due to the quantum confinement effect [37].

In order to clarify the mechanism of stimulated emission of these MQWs, the temperature dependence of the stimulated-emission spectrum in the temperature range from low temperature to room temperature was estimated. Figure 11 shows the temperature dependence of the peak energy of the stimulated emission band in the QWs (Mg concentration of 0.12, L_w s of 37.0 \AA and 17.5 \AA). For comparison, the same plot for thin films of ZnO grown on sapphire substrates is shown in Fig. 11(a). It is already clear that the RT stimulated emission band in these thin films is what is called the P -line, which one of the typical phenomena of high-density exciton effects. Inelastic scattering between excitons (Auger-like process) gives rise to the appearance of this stimulated emission band. One of the two excitons participating in the collisional events is ionized, whereas the other is recombined radiatively after collision. At sufficiently low temperatures, peak energy of the relevant stimulated emission band is lower than the resonance energy of an exciton, the energy difference of which is equal to the EBE. The temperature dependence of the peak energy difference in QWs shows the same behavior as that of ZnO, as can be clearly understand in Fig. 11. Thus, as a result of careful comparison with that of a ZnO thin film, it became clear that the mechanism of this stimulated emis-

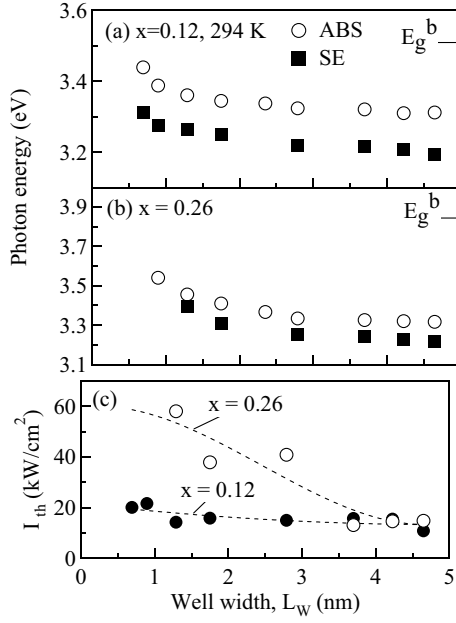


Figure 9: Optical transition energies of subband absorption (open circles) and stimulated emission (closed squares) as a function of well layer thickness (L_w) for ZnO/Mg_xZn_{1-x}O MQWs with $x=0.12$ (a) and $x=0.26$ (b). Band gap energy of the barrier layers (E_g^b) is also shown. (c) L_w dependence of the stimulated emission threshold (I_{th}) in MQWs with $x=0.12$ (closed circles) and $x=0.26$ (open circles). Stimulated emission did not occur for the $x=0.26$ films with L_w below 1 nm since the excitation energy is lower than the absorption energy [36].

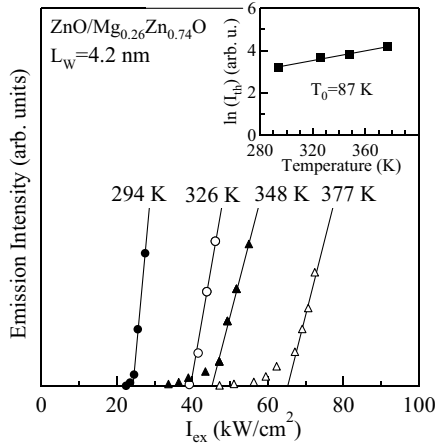


Figure 10: Temperature dependence of emission intensity as a function of excitation intensity (I_{ex}) in a ZnO/Mg_{0.26}Zn_{0.74}O SL ($L_w = 4.2$ nm). Inset shows the threshold intensity (I_{th}) as a function of temperature on a logarithmic scale [36].

sion is inelastic scattering processes between the excitons. Therefore, the L_w dependence of EBEs can be experimentally determined from analysis of the energy position of the P -line. As shown in Fig. 5 (right axis), when L_w decreased, the EBE increased up to about 90 meV and exceeded $\hbar\omega_{LO}$ (72 meV). This enhancing effect is due to the quantum confinement effect. It has been revealed that these estimated EBEs approximately agree with the theoretical values [27, 31]. If QW structures were used, the phonon scattering process and thermo-broadening effect of excitonic linewidth can be controlled. These are favorable from the viewpoint of application.

Combinatorial concept-aided techniques adopted in the growth of our samples suppressed the variations in crystal growth conditions and hence the undesired uncertainty in the deduced spectroscopic results. In a related review article, the benefit of the combinatorial technique is described in detail [13]. For example, the well width dependence of the radiative and nonradiative recombination times of localized excitons was estimated by time-resolved photoluminescence spectroscopy [38, 33]. Well width dependence of *biexciton* binding energy was also estimated [39]. In addition, optical properties of (Cd,Zn)O/(Mg,Zn)O MQWs have not ever explored so far except our work [33]. These structures are advantageous from the viewpoint of almost perfect in-plane lattice-matching.

8 Conclusions

If a short-wavelength (UV region) semiconductor laser using exciton transitions in low-dimensional crystals (e.g., quantum wells) of ZnO can be produced, it is expected that threshold of the laser action will become lower than that of a laser using an ordinary recombination mechanism of electrons and holes. This study has shown, through experiments on optical excitation, that it is possible to produce a laser with a low threshold (i.e., small driving current density). Laser action due to the effect of a longitudinal cavity using grain boundaries is no longer observed in ZnO epitaxial layers deposited on lattice-matched substrates, because their level of crystallinity has been greatly improved.

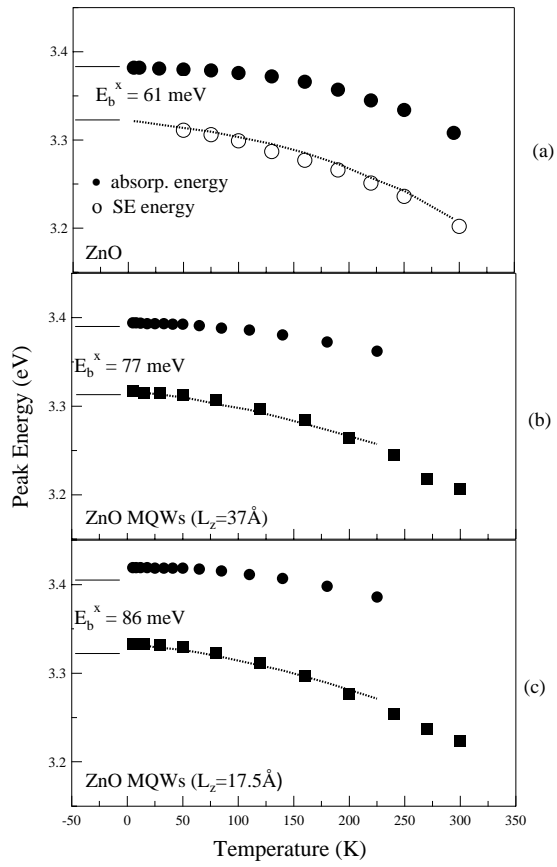


Figure 11: Temperature dependence of peak energy of the P band (open circles) and free exciton energy (filled circles) in a ZnO epitaxial layer (a) and in ZnO/Zn_{0.88}Mg_{0.12}O MQWs (b) and (c) [37].

Moreover, they no longer show a polycrystalline nature (i.e., assembly of hexagonal pillar prisms). The corresponding resonance cavity structure has disappeared.

Moreover, a p - n junction is essential for the production of a current injection laser. A ZnO crystal usually shows n -type conductivity and it has not been possible to produce a p -type layer with low resistance. Such a feature of widegap semiconductors is called unipolarity in carrier doping. In this chapter, we have not discussed this problem.

Such high-quality ZnO QWs deposited on lattice-matched substrates are expected to have many applications for UV optoelectronics devices. Various applications of ZnO, such as its use in transparent electric-conduction films or a surface acoustic-wave device, are well-known. New function of this substance have been found through research on high-quality single-crystalline thin films grown by the use of the laser-assisted molecular-beam-epitaxy. New physical properties of other oxides may also be discovered in the future.

Acknowledgements

The quantum wells used as the target of optical characterization in our study were produced by Dr. A. Ohtomo and K. Tamura using equipment originally constructed by Dr. Y. Matsumoto, Tokyo Institute of Technology, Japan. We would like to express our gratitude to the abovementioned researchers as well as Dr. Ngyuen Tien Tuan, Dr. H. D. Sun and C. H. Chia, Institute of Physical and Chemical Research, Japan, for their assistance in all aspects of our research.

References

- [1] Hiromitsu Sakai, Takashi Koide, Hiroyuki Suzuki, Machiko Yamaguchi, Shiro Yamasaki, Masayoshi Koike, Hiroshi Amano, and Isamu Akasaki. GaN/GaInN/GaN double heterostructure light emitting diode fabricated using plasma-assisted molecular beam epitaxy. *Jpn. J. Appl. Phys. Part 2*, 34(11A):L1429–L1431, November 1995.
- [2] S. Nakamura, S. Pearton, and G. Fasol. *The Blue Laser Diode*. Springer-Verlag Berlin, 2000.
- [3] A. Ohtomo, M. Kawasaki, T. Koida, K. Masubuchi, H. Koinuma, Y. Sakurai, Y. Yoshida, T. Yasuda, and Y. Segawa. $\text{Mg}_x\text{Zn}_{1-x}\text{O}$ as a II-IV widegap semiconductor alloy. *Appl. Phys. Lett.*, 72(19):2466, May 1998.
- [4] M. Kawasaki, A. Ohtomo, R. Shiroki, I. Ohkubo, H. Kimura, G. Isoya, T. Yasuda, Y. Segawa, and H. Koinuma. ZnO quantum structures towards UV diode lasers. In *Extended Abstracts of the 1998 International Conference on Solid State Devices and Materials*, page 356, Hiroshima, Japan, 1998. Business Ctr. Acad. Soc. Jpn.
- [5] T. Makino, Y. Segawa, M. Kawasaki, A. Ohtomo, R. Shiroki, K. Tamura, T. Yasuda, and H. Koinuma. Band gap engineering based on (Mg,Zn)O and (Cd,Zn)O ternary alloy films. *Appl. Phys. Lett.*, 78(9):1237, Feb. 2001.
- [6] A. Ohtomo, M. Kawasaki, I. Ohkubo, H. Koinuma, T. Yasuda, and Y. Segawa. Structure and optical properties of ZnO/Mg_{0.2}Zn_{0.8}O superlattices. *Appl. Phys. Lett.*, 75(1):980, 1999.
- [7] A. Ohtomo, R. Shiroki, I. Ohkubo, H. Koinuma, and M. Kawasaki. Thermal stability of supersaturated $\text{Mg}_x\text{Zn}_{1-x}\text{O}$ alloy films and $\text{Mg}_x\text{Zn}_{1-x}\text{O}/\text{ZnO}$ heterointerfaces. *Appl. Phys. Lett.*, 75(26):4088, Dec. 1999.
- [8] T. Makino, Y. Segawa, A. Ohtomo, K. Tamura, T. Yasuda, M. Kawasaki, and H. Koinuma. Strain effect on exciton resonance energies of zno epitaxial layers. *Appl. Phys. Lett.*, 79(9):1282, August 2001.
- [9] N. Kimizuka and T. Mohri. *J. Solid State Chem.*, 78:98, 1989.
- [10] A. Ohtomo, K. Tamura, K. Saikusa, T. Takahashi, T. Makino, Y. Segawa, H. Koinuma, and M. Kawasaki. Single crystalline ZnO films grown on lattice matched $\text{ScAlMgO}_4(0001)$ substrates. *Appl. Phys. Lett.*, 75(17):2635, 1999.
- [11] Several efforts to grow not MQWs but epilayers are currently being made using MgO or $\text{MgAl}_2\text{O}_4(111)$ substrates by means of plasma-assisted MBE, whose misfits are smaller than that of sapphire (Y. F. Chen et al).
- [12] Y. Matsumoto, M. Murakami, Z. W. Jin, A. Ohtomo, M. Lippmaa, M. Kawasaki, and H. Koinuma. Combinatorial laser molecular epitaxy (MBE) growth of Mg-Zn-O alloy for band gap engineering. *Jpn. J. Appl. Phys., Part2*, 38(2(6A/B)):L603, Jun. 1999.
- [13] H. Koinuma, H. N. Aiyer, and Y. Matsumoto. Combinatorial solid state materials science and technology. *Sci. & Tech. Adv. Mater.*, 1(1):1, 2000.
- [14] A. Ohtomo, T. Makino, K. Tamura, Y. Matsumoto, Y. Segawa, Z. K. Tang, G. K. L. Wang, H. Koinuma, and M. Kawasaki. High throughput optimizations of alloy and doped films based on ZnO and parallel synthesis of ZnO/(Mg,Zn)O quantum wells using combinatrial laser MBE towards ultraviolet laser. *Proceedings of SPIE*, 3941:70, 2000.

- [15] T. Makino, G. Isoya, Y. Segawa, C. H. Chia, T. Yasuda, M. Kawasaki, A. Ohtomo, K. Tamura, Y. Matsumoto, and H. Koinuma. Optical characterization for combinatrial system based on semiconductor ZnO. In G. Jabbour, editor, *Proceedings of the 1st International Conference on Combinatorial and Composition Spread Techniques in Material and Device Development, San Jose*, volume 3941, page 28, Bellingham, 2000. SPIE.
- [16] M. Ohtani, T. Fukumura, M. Kawasaki, K. Omote, T. Kikuchi, J. Harada, A. Ohtomo, M. Lippmaa, T. Ohnishi, D. Komiyama, R. Takahashi, Y. Matsumoto, and H. Koinuma. Concurrent x-ray diffractometer for high throughput structural diagnosis of epitaxial thin films. *Appl. Phys. Lett.*, 79(22):3594, Nov. 2001.
- [17] M. Ohtani, T. Fukumura, M. Kawasaki, K. Omote, T. Kikuchi, J. Harada, and H. Koinuma. Concurrent evaluation of strain in heteroepitaxial thin films with continuous lattice mismatch spread. *Appl. Phys. Lett.*, 80(12):2066, Mar. 2002.
- [18] T. Makino, K. Tamura, C. H. Chia, Y. Segawa, M. Kawasaki, A. Ohtomo, and H. Koinuma. Optical properties of zno:al epilayers: Observation of room-temperature many-body absorption-edge singularity. *Phys. Rev. B*, 65(12):121201(R), March 2002.
- [19] E. Mollwo. In O. Madelung, M. Schulz, and H. Weiss, editors, *Semiconductors: Physics of II-VI and I-VII Compounds, Semimagnetic Semiconductors*, volume 17 of *Landolt-Börnstein New Series*, page 35. Springer, Berlin, 1982.
- [20] W. Y. Liang and A. D. Yoffe. Transmission spectra of ZnO single crystals. *Phys. Rev. Lett.*, 20(2):59, 1968.
- [21] T. Makino, C. H. Chia, N. T. Tuan, Y. Segawa, M. Kawasaki, A. Ohtomo, K. Tamura, and H. Koinuma. Exciton spectra in ZnO epitaxial layers on lattice-matched substrates grown with laser-molecular-beam epitaxy. *Appl. Phys. Lett.*, 76(24):3549, Jun. 2000.
- [22] Akira Ohtomo. *Quantum structures and ultraviolet light-emitting devices based on ZnO thin films grown by laser molecular-beam epitaxy*. PhD thesis, Tokyo Institute of Technology, Mar. 2000.
- [23] A. Ohtomo, M. Kawasaki, Y. Sakurai, I. Ohkubo, R. Shiroki, Y. Yoshida, Y. Sakurai, T. Yasuda, Y. Segawa, and H. Koinuma. Fabrication of alloys and superlattices based on zno towards ultraviolet laser. *Mat. Sci. Eng. B*, 56(2):263, Nov. 1998.
- [24] T. Makino, N. T. Tuan, H. D. Sun, C. H. Chia, Y. Segawa, M. Kawasaki, A. Ohtomo, K. Tamura, and H. Koinuma. Room-temperature luminescence of excitons in ZnO/(Mg,Zn)O multi-quantum wells on lattice-matched substrates. *Appl. Phys. Lett.*, 77(7):975, 2000.
- [25] I. I. Gol'dman and V. Krivchenokov. *Problems of Quantum Mechanics*, page 60. Addison-Wesley, Reading, Mass., 1961.
- [26] K. Hümmer. Interband magnetoreflexion in ZnO bulk. *Phys. Status Solidi*, 56:249, 1973.
- [27] Giuliano Coli and K. K. Bajaj. Excitonic transitions in zno/mgzno quantum well heterostructures. *Appl. Phys. Lett.*, 78(19):2861, May 2001.
- [28] P. Lautenschlager, M. Garriga, S. Logothetidis, and M. Cardona. Interband critical points of GaAs and their temperature dependence. *Phys. Rev. B*, 35:9174, 1987.

- [29] N. T. Pelekanos, J. Ding, M. Hagerott, A. V. Nurmikko, H. Luo, N. Samarth, and J. K. Furdyna. Quasi-2-dimensional (Zn,Cd)Se/ZnSe quantum wells reduced exciton lo-phonon coupling due to confinement effects. *Phys. Rev. B*, 45:6037, 1992.
- [30] H. D. Sun, T. Makino, N. T. Tuan, Y. Segawa, M. Kawasaki, A. Ohtomo, K. Tamura, and H. Koinuma. Temperature dependence of the exciton linewidth in ZnO/(Mg,Zn)O multi-quantum wells. *Appl. Phys. Lett.*, 78(17):2464, 2001.
- [31] H. D. Sun, T. Makino, Y. Segawa, M. Kawasaki, A. Ohtomo, K. Tamura, and H. Koinuma. Enhancement of exciton binding energies in zno/znmgo multiquantum wells. *J. Appl. Phys.*, 91(4):1993, Feb. 2002.
- [32] T. Makino, N. T. Tuan, H. D. Sun, C. H. Chia, Y. Segawa, M. Kawasaki, A. Ohtomo, K. Tamura, M. Baba, H. Akiyama, T. Suemoto, S. Saito, T. Tomita, and H. Koinuma. Temperature dependence of near ultraviolet photoluminescence in ZnO/(Mg,Zn)O multi-quantum wells. *Appl. Phys. Lett.*, 78(14):1979, 2001.
- [33] T. Makino, N. T. Tuan, Y. Segawa, C. H. Chia, M. Kawasaki, A. Ohtomo, K. Tamura, and H. Koinuma. Radiative and nonradiative recombination processes in lattice-matched (Cd,Zn)O/(Mg,Zn)O multiquantum wells. *Appl. Phys. Lett.*, 77(11):1632, 2000.
- [34] C. Gourdon and P. Lavallard. Exciton transfer between localized states in CdSSe alloys. *Phys. Status Solidi (b)*, 153:641, 1989.
- [35] C. Yong-Hoon, B. D. Little, G. H. Gainer, J. J. Song, S. Keller, U. K. Mishra, and S. P. DenBaars. Carrier dynamics of abnormal temperature-dependent emission shift in mocvd-grown ingan epilayers and ingan/gan quantum wells. *MRS Int. J. Nitride. Res.*, 4S1:G2.4, 1999.
- [36] A. Ohtomo, K. Tamura, M. Kawasaki, T. Makino, Y. Segawa, Z. K. Tang, G.K.L. Wong, Y. Matsumoto, and H. Koinuma. Room-temperature stimulated emission of excitons in ZnO/(Mg,Zn)O superlattices. *Appl. Phys. Lett.*, 77(14):2204, Oct. 2000.
- [37] H. D. Sun, T. Makino, N. T. Tuan, Y. Segawa, Z. K. Tang, G. K. L. Wong, M. Kawasaki, A. Ohtomo, K. Tamura, and H. Koinuma. Stimulated emission induced by the inelastic exciton-exciton scattering in ZnO/(Mg,Zn)O multi-quantum wells. *Appl. Phys. Lett.*, 77(26):4250, 2000.
- [38] C. H. Chia, T. Makino, Y. Segawa, M. Kawasaki, A. Ohtomo, K. Tamura, and H. Koinuma. Well-width dependence of radiative and nonradiative recombination times in zno/mgzno multiple quantum wells. *J. Appl. Phys.*, 90(7):3650, Nov. 2001.
- [39] H. D. Sun, T. Makino, Y. Segawa, M. Kawasaki, A. Ohtomo, K. Tamura, and H. Koinuma. Biexciton emission from ZnO/(Mg,Zn)O multi-quantum wells. *Appl. Phys. Lett.*, 78(22):3385, May 2001.